DALTON
FULL PAPER

# Mixed inorganic–organic anion frameworks: synthesis and characterisation of $[Mn_4(PO_4)_2(C_2O_4)(H_2O)_2]$ and $[H_3N(CH_2)_3NH_3][Mn_2(HPO_4)_2(C_2O_4)(H_2O)_2]$

**Zoe A. D. Lethbridge,[a] Adrian D. Hillier,[b] Robert Cywinski[b] and Philip Lightfoot *[a]**

[a] *School of Chemistry, University of St Andrews, Purdie Building, North Haugh, St Andrews, Fife, UK KY16 9ST*

[b] *School of Physics and Astronomy, University of St Andrews, North Haugh, St Andrews, Fife, UK KY16 9SS. E-mail: pl@st-and.ac.uk*

***Received 17th January 2000, Accepted 24th March 2000***
***Published on the Web 19th April 2000***

Two new three-dimensional manganese phosphate oxalate frameworks have been synthesized and their structures determined by single crystal X-ray diffraction. The compound $[Mn_4(PO_4)_2(C_2O_4)(H_2O)_2]$ **1** is monoclinic, space group $P2_1/c$, $a = 10.263(3)$, $b = 6.526(2)$, $c = 10.082(3)$ Å and $\beta = 116.84(2)°$. $MnO_5$ and $MnO_6$ polyhedra share edges to form tetramers, which are further linked by $PO_4$ tetrahedra to form layers in the *bc* plane. The layer, which contains an extended array of direct Mn–O–Mn linkages, is in turn linked to neighbouring layers by pillaring bisbidentate oxalate groups. Magnetisation measurements indicate antiferromagnetic interactions, and suggest that the material may be a two dimensional antiferromagnet. Thermogravimetric analysis shows the structure to be stable up to 240 °C. The compound $[H_3N(CH_2)_3NH_3][Mn_2(HPO_4)_2(C_2O_4)(H_2O)_2]$ **2** is monoclinic, space group $P2_1/n$, $a = 5.474(2)$, $b = 15.737(2)$, $c = 9.056(2)$ Å, $\beta = 93.47(3)°$, and includes a disordered 1,3-diaminopropane dication in channels parallel to the *a* direction. In contrast to **1**, no direct Mn–O–Mn linkages occur.

## Introduction

The field of open framework materials is currently a diverse and active one. The initial work on aluminosilicates (zeolites) and aluminophosphates ($AlPO_4$s) has produced materials with channel and cage systems of various dimensionality and size.[1] Often templates or space filling species, usually protonated amines, are used to control the shapes and sizes of the channels. Zeolites and $AlPO_4$s have good thermal stability, allowing the template molecules to be removed, leaving the channels empty. The materials may then be useful in areas such as shape selective catalysis or adsorption.[2] Transition metals may be substituted into the framework,[3] or alternatively aluminium may be dispensed with altogether, to produce transition metal phosphate frameworks.[4–7]

Another rapidly expanding area is metal organic frameworks. These co-ordination polymers, which may be one-, two-, or three-dimensional, are formed from transition metal centres which co-ordinate to ligands with several donor atoms, usually oxygen or nitrogen.[8–12] Stability of the framework on removal of space filling species, whilst more difficult in these systems, has been demonstrated.[13] The potential for synthesizing new metal organic frameworks lies partly in the huge number of molecules available to act as ligands in such systems. In contrast the diversity of zeolite and $AlPO_4$ frameworks is in the main due to development of new templates.[14,15]

We aim to combine this flexibility of metal organic co-ordination systems with the thermal stability of the phosphate materials to produce new open frameworks. We have made use of the rigid oxalate ligand which has four potential donor sites for metal co-ordination, along with phosphate units to bridge metal centres. These two species have previously been shown to produce frameworks with a number of different metals. In the iron phosphate oxalate system several structures have been reported: $[Fe_4(PO_4)_2(C_2O_4)(H_2O)]$,[16] $[Fe_2(PO_4)(C_2O_4)_{0.5}(H_2O)]$, $[N_2C_4H_{12}]_{0.5}[Fe_2(HPO_4)(C_2O_4)_{1.5}]$,[17] $[NH_3(CH_2)_2NH_3]_{1.5}[Fe_3(PO_4)(HPO_4)_3(C_2O_4)_{1.5}]\cdot xH_2O$,[18] $[C_4H_{12}N_2][Fe_4(HPO_4)_2(C_2O_4)_3]$ and $[C_5H_{14}N_2][Fe_2(HPO_4)_3(C_2O_4)]$.[19] Group 13 elements have also been utilised in $[H_3N(CH_2)_2NH_3]_{2.5}[Al_4H(HPO_4)_4(H_2PO_4)_2(C_2O_4)_4]$,[20] $[Ga_5(OH)_2(C_{10}H_9N_2)(PO_4)_4(C_2O_4)]\cdot 2H_2O$[21] and $[C_4H_{12}N_2][In_2(HPO_4)_3(C_2O_4)]\cdot H_2O$.[22] Here we report the synthesis and crystal structure determination of $[Mn_4(PO_4)_2(C_2O_4)(H_2O)_2]$ **1** and $[H_3N(CH_2)_3NH_3][Mn_2(HPO_4)_2(C_2O_4)(H_2O)_2]$ **2**, and thermogravimetric analysis and magnetic susceptibility of **1**.

## Experimental

### Synthesis of $[Mn_4(PO_4)_2(C_2O_4)(H_2O)_2]$ 1

The compound $MnC_2O_4\cdot 2H_2O$ (0.5272 g, 2.95 mmol) was added to water (10 ml) with stirring, followed by $(NH_4)_2HPO_4$ (0.1976 g, 1.50 mmol) resulting in a pH of 6, and the mixture washed into a Teflon-lined steel autoclave with 5 ml of water (approx. ratio $MnC_2O_4\cdot 2H_2O : (NH_4)_2HPO_4$ : water 2 : 1 : 555). The mixture was heated at 160 °C for 48 hours, cooled in air, filtered and washed with distilled water and air-dried (final pH 6). 0.3397 g (86.30% yield on Mn) of pink diamond shaped crystals was obtained (Found: C, 4.66; H, 0.76. $Mn_4(PO_4)_2(C_2O_4)(H_2O)_2$ requires C, 4.50; H, 0.76%).

### Synthesis of $[H_3N(CH_2)_3NH_3][Mn_2(HPO_4)_2(C_2O_4)(H_2O)_2]$ 2

The compound $Mn_2O_3$ (0.3279 g, 2.077 mmol) was added to water (15 ml) with stirring, followed by $H_3PO_4$ (85%, 0.23 ml, 1.993 mmol), $HO_2CCO_2H$ (0.2567 g, 2.036 mmol) and $H_2N(CH_2)_3NH_2$ (0.17 ml, 2.036 mmol) resulting in a pH of 2 (approx. ratio $Mn_2O_3 : H_3PO_4 : HO_2CCO_2H : H_2N(CH_2)_3NH_2$ : water 1 : 1 : 1 : 1 : 417). The mixture was heated in a Teflon-lined steel autoclave at 120 °C for 48 hours, then air-cooled. The resulting mixture (pH 6) was filtered, washed with distilled water and dried in air giving 0.4082 g of a mixture of colourless

DOI: 10.1039/b000449i

**Table 1** Crystal data and details of structure solution and refinement for compounds **1** and **2**

| | **1** | **2** |
|---|---|---|
| Formula | $[Mn_4(PO_4)_2(C_2O_4)(H_2O)_2]$ | $[H_3N(CH_2)_3NH_3][Mn_2(HPO_4)_2(C_2O_4)(H_2O)_2]$ |
| Formula weight | 533.745 | 502.026 |
| Crystal system | Monoclinic | Monoclinic |
| Space group | $P2_1/c$ | $P2_1/n$ |
| $a$/Å | 10.263(3) | 5.474(2) |
| $b$/Å | 6.526(2) | 15.737(2) |
| $c$/Å | 10.082(3) | 9.056(2) |
| $\beta$/° | 116.84(2) | 93.47(3) |
| $V$/Å$^3$ | 602.8(4) | 778.7(3) |
| $Z$ | 2 | 2 |
| $\mu$(Mo-K$\alpha$)/cm$^{-1}$ | 4.438 | 1.906 |
| Total reflections | 1496 | 1439 |
| Observed reflections ($I > 3\sigma(I)$) | 1240 | 1094 |
| $R$, $R_w$ | 0.0314, 0.0350 | 0.0408, 0.0388 |

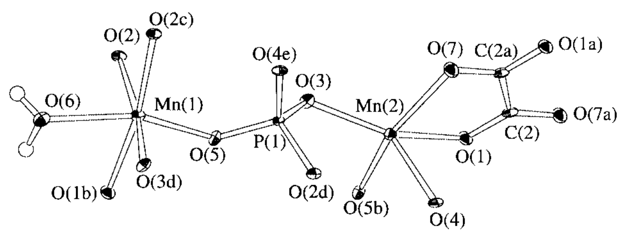


**Fig. 1** Building unit of compound **1** showing the atom labelling scheme. Thermal ellipsoids are shown at 50% probability. Symmetry labels: a, $1 - x$, $2 - y$, $2 - z$; b, $-x$, $2 - y$, $1 - z$; c, $-x$, $2 - y$, $-z$; d, $-x$, $y - \frac{1}{2}$, $\frac{1}{2} - z$; e, $x$, $\frac{3}{2} - y$, $z - \frac{1}{2}$.

crystals and $Mn_2O_3$ (JCPDS 24-508, identified by powder X-ray diffraction).

### Characterisation

Magnetisation measurements were obtained on a 0.2119 g polycrystalline sample of $[Mn_4(PO_4)_2(C_2O_4)(H_2O)_2]$ using an Oxford Instruments Vibrating Sample Magnetometer in a field of 4 Tesla over the temperature range 4–170 K. The temperature dependent susceptibility of the sample was derived assuming linearity of the magnetisation with applied field.

Thermogravimetric analysis (TGA) was carried out on a TA Instruments SDT 2960 simultaneous DTA–TGA furnace, from room temperature to 800 °C at a heating rate of 10 °C min$^{-1}$ under both nitrogen and oxygen.

X-Ray data collection for compounds **1** and **2** was carried out at 25 °C on a Rigaku AFC7S four circle diffractometer using graphite monochromated Mo-K$\alpha$ radiation ($\lambda = 0.71073$ Å). Unit cell parameters were determined from a least squares refinement of the setting angles of 25 reflections in the range $15 < 2\theta < 25°$. Crystallographic details are given in Table 1. Structure solution and refinement were carried out using the SIR 92[23] and TEXSAN[24] suites.

CCDC reference number 186/1910.

See http://www.rsc.org/suppdata/dt/b0/b000449i/ for crystallographic files in .cif format.

## Discussion

The compound $[Mn_4(PO_4)_2(C_2O_4)(H_2O)_2]$ **1** is a three dimensional framework constructed from $MnO_5$, $MnO_6$ and $PO_4$ polyhedra and oxalate units. The building unit is shown in Fig. 1, selected bond lengths and angles in Table 2. There are two different types of manganese in the structure, both in the 2+ oxidation state as indicated by bond valence calculations:[25] Mn(1) 2.050, Mn(2) 1.881. Mn(1) exists in a distorted octahedron, while Mn(2) is five-co-ordinate. (The sixth oxygen, O(6), is at a distance of 2.555(3) Å from Mn(2).) Each Mn(1) is co-ordinated to one oxalate oxygen, four phosphate oxygens and a water molecule. Mn(2) is co-ordinated to both oxalate oxygens and three phosphate oxygens. The smallest O–Mn(2)–O angle (75.1°) is due to the bidentate oxalate co-ordination. Two $Mn(1)O_6$ and two $Mn(2)O_5$ polyhedra share edges to form a tetranuclear building unit, illustrated in Fig. 2. These units are linked to each other *via* corner sharing of the manganese polyhedra, and also by corner sharing phosphate tetrahedra, to form manganese phosphate layers in the *bc* plane.

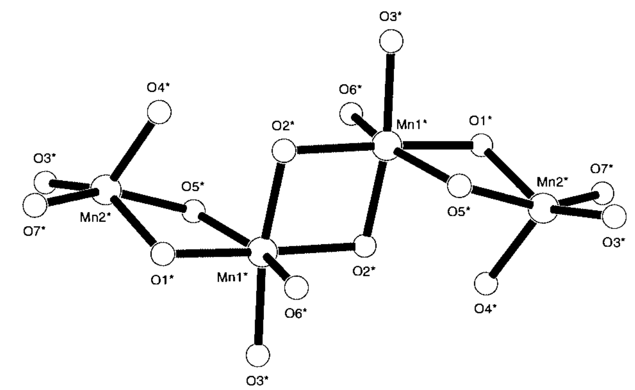


**Fig. 2** Tetranuclear building unit of compound **1** showing edge-sharing $MnO_5$ and $MnO_6$ polyhedra.

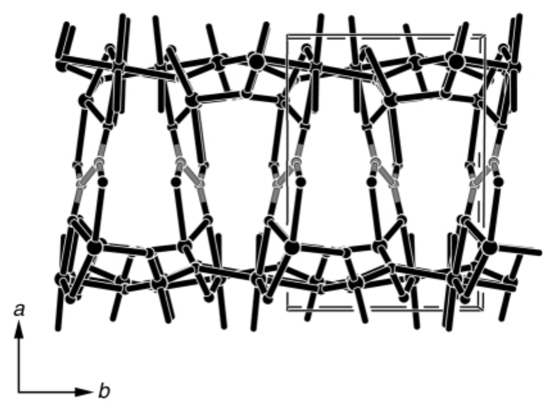


**Fig. 3** A skeletal *ab* projection of compound **1** showing the oxalate anions bridging two manganese phosphate layers.

Oxalate units show bismonodentate co-ordination to Mn(1) and bisbidentate co-ordination to Mn(2), acting as pillars between adjacent manganese phosphate layers to produce the extended three dimensional network. The *ab* projection of the structure (Fig. 3) shows a small amount of open space between the oxalate pillars. The Mn(1) co-ordination sphere is completed by a water molecule, indicated by the low bond valence of O(6) (0.2800). Hydrogen bonding is possible between the water and the framework oxygens (see Table 2).

**Table 2** Selected bond lengths (Å) and angles (°) for compound **1**

| | | | |
|---|---|---|---|
| Mn(1)–O(1) | 2.253(3) | Mn(2)–O(1) | 2.214(3) |
| Mn(1)–O(2) | 2.142(3) | Mn(2)–O(3) | 2.120(3) |
| Mn(1)–O(2) | 2.219(3) | Mn(2)–O(4) | 2.127(3) |
| Mn(1)–O(3) | 2.121(3) | Mn(2)–O(5) | 2.126(3) |
| Mn(1)–O(5) | 2.153(3) | Mn(2)–O(7) | 2.181(3) |
| Mn(1)–O(6) | 2.261(3) | | |
| O(1)–Mn(1)–O(2) | 93.0(1) | O(1)–Mn(2)–O(3) | 149.0(1) |
| O(1)–Mn(1)–O(2) | 171.3(1) | O(1)–Mn(2)–O(4) | 81.8(1) |
| O(1)–Mn(1)–O(3) | 91.9(1) | O(1)–Mn(2)–O(5) | 78.8(1) |
| O(1)–Mn(1)–O(5) | 77.4(1) | O(1)–Mn(2)–O(7) | 75.1(1) |
| O(1)–Mn(1)–O(6) | 78.1(1) | O(3)–Mn(2)–O(4) | 128.6(1) |
| O(2)–Mn(1)–O(2) | 82.1(1) | O(3)–Mn(2)–O(5) | 93.8(1) |
| O(2)–Mn(1)–O(3) | 168.8(1) | O(3)–Mn(2)–O(7) | 105.4(1) |
| O(2)–Mn(1)–O(5) | 86.8(1) | O(4)–Mn(2)–O(5) | 89.8(1) |
| O(2)–Mn(1)–O(6) | 89.3(1) | O(4)–Mn(2)–O(7) | 92.4(1) |
| O(2)–Mn(1)–O(3) | 91.8(1) | O(5)–Mn(2)–O(7) | 153.3(1) |
| O(2)–Mn(1)–O(5) | 109.3(1) | | |
| O(2)–Mn(1)–O(6) | 94.6(1) | | |
| O(3)–Mn(1)–O(5) | 104.1(1) | | |
| O(3)–Mn(1)–O(6) | 81.8(1) | | |
| O(5)–Mn(1)–O(6) | 155.0(1) | | |

Hydrogen bonds

| A | H | B | A–H | H···B (Å) | A···B (Å) | A–H···B |
|---|---|---|---|---|---|---|
| O(6) | H(1) | O(7) | 0.92(5) | 1.92(5) | 2.825(4) | 166(5) |
| O(6) | H(2) | O(4) | 0.83(6) | 2.04(6) | 2.790(4) | 150(6) |

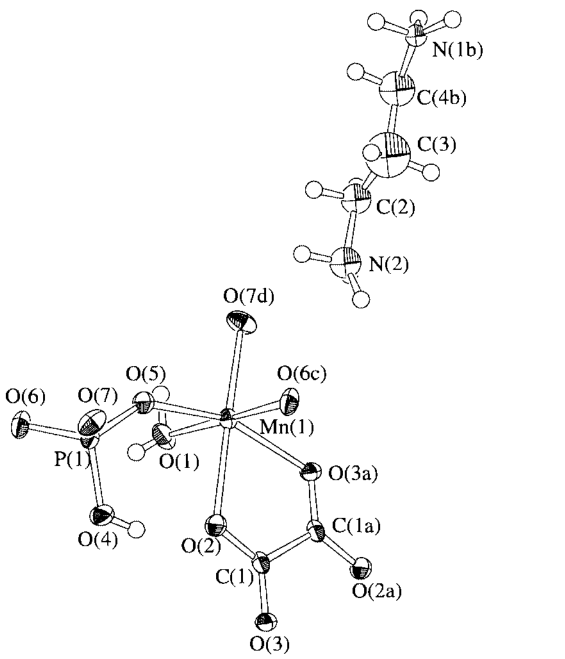


**Fig. 4** Building unit of compound **2** showing the atom labelling scheme. Thermal ellipsoids are at 50% probability; only one position of the disordered 1,3-diaminopropane cation is shown. Symmetry labels: a, $1 - x, -y, 2 - z$; b, $2 - x, 1 - y, 2 - z$; c, $1 + x, y, z$; d, $\frac{1}{2} + x, \frac{1}{2} - y, z - \frac{1}{2}$.

The compound $[H_3N(CH_2)_3NH_3][Mn_2(HPO_4)_2(C_2O_4)(H_2O)_2]$ **2** is also a three dimensional framework, constructed from $MnO_6$ octahedra, $PO_4$ tetrahedra and oxalate units, and contains diprotonated 1,3-diaminopropane in one dimensional channels in the *a* direction. The building unit is shown in Fig. 4, selected bond lengths and angles in Table 3. There is one type of manganese in the structure, confirmed as $Mn^{2+}$ by bond valence calculations[25] (calc. 2.063), which exists in a distorted $MnO_6$ octahedron. The co-ordination sphere consists of one water molecule, two oxalate oxygens and three phosphate oxygens. The distortion is caused by the bidentate oxalate co-ordination, resulting in an O–Mn–O angle of 73.2°. The $PO_4$ tetrahedra are connected to $MnO_6$ octahedra at three vertices and an $OH^-$ group is found on the fourth. The presence of the water and hydroxyl hydrogen atoms may be inferred by the oxygen bond valence sums; 0.27 for O(1) (*i.e.* $OH_2$) and 1.07 for O(4) (*i.e.* OH). These three hydrogen atoms were located and refined isotropically. The diprotonated 1,3-diaminopropane is disordered over two positions, with the central carbon atom C(3) lying on an inversion centre. The positions of the hydrogen atoms on the carbon and nitrogen were geometrically fixed.

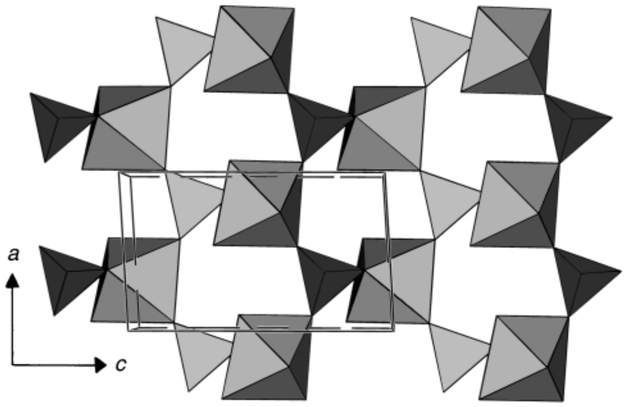


**Fig. 5** *ac* Projection of compound **2**. Chains of $MnO_6$ and $PO_4$ polyhedra run in the *a* direction. These are connected into sheets by further $MnO_6$–$PO_4$ corner sharing.

Chains are formed in the *a* direction from alternating $MnO_6$ octahedra and $PO_4$ tetrahedra which share corners. The chains are connected to each other *via* a third corner on both the $MnO_6$ octahedra and $PO_4$ tetrahedra, forming sheets in the *ac* plane (Fig. 5). Thus each octahedron is connected to three tetrahedra and *vice versa*. There are no Mn–O–Mn linkages in this structure, in contrast to **1**.

Bisbidentate oxalate anions co-ordinate to manganese centres in adjacent layers, producing the three-dimensional structure (Fig. 6). Channels are found in the *a* direction between these oxalate pillars, which contain diprotonated 1,3-diaminopropane, disordered over two positions. The cations are hydrogen bonded to the framework *via* N–H···O bonds; hydrogen bonding is also seen between the $H_2O$ and OH groups and the oxalate oxygens (see Table 3).

### Thermogravimetric analysis

TGA of compound **1** was carried out from room temperature to 800 °C at 10 °C $min^{-1}$ in both $N_2$ (Fig. 7a) and $O_2$ (Fig. 7b). Under $N_2$ the loss can be split up into three steps, although these are not well separated. The first (240–448 °C), which is endothermic, can be attributed to loss of water (observed 6.412%, $2H_2O$ calc. 6.75%). Between 448 and 800 °C a further 13.36% is lost in two exothermic steps, resulting in a brown powder containing $Mn_3(PO_4)_2$ (JCPDS 40–112) and $Mn_3O_4$ (JCPDS 18–803, 24–734) identified by powder X-ray diffraction. This may be accounted for by decomposition of the oxalate to a mixture of CO and $CO_2$. The mass lost is 13.36%, compared to 10.50% calc. for 2CO and 16.49% calc. for $2CO_2$. A similar weight loss profile is obtained under $O_2$, however there is a plateau between the second and third steps. A sample heated to 485 °C, where the second step finishes, gives a largely amorphous black material which shows some peaks in the X-ray powder pattern, thought to be $Mn_2P_2O_7$ (JCPDS 29–891, 35–1497). The weight loss begins at 242 °C, by 800 °C the total weight loss was 19.67%, resulting in a black powder containing $Mn_3(PO_4)_2$ (JCPDS 40–112) as before. The first two steps in the process are exothermic (5.765, 2.870%), followed by a slight endotherm in the third (11.04%). A similar water loss and oxalate decomposition is thought to occur in this case, possibly

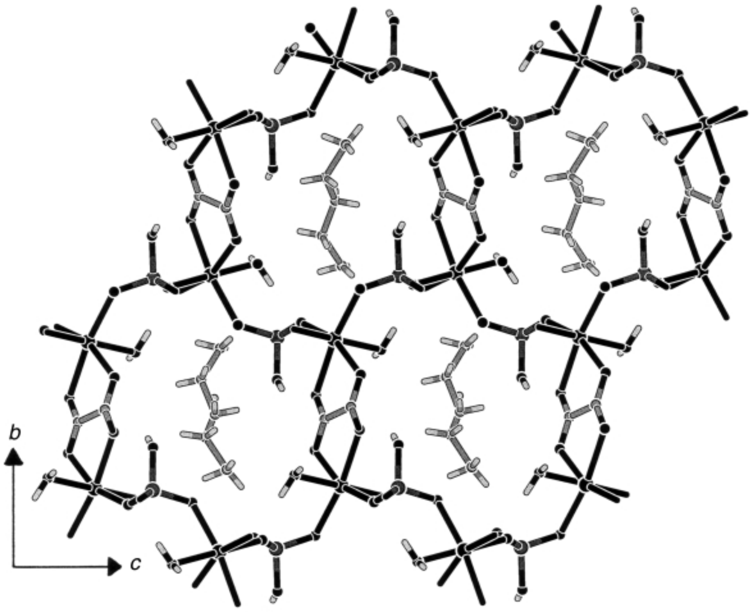


**Fig. 6** A *bc* projection of compound **2** showing one position of the disordered 1,3-diaminopropane cation in the channels parallel to *a*.

**Table 3** Selected bond lengths (Å) and angles (°) for compound **2**

| | | | |
|---|---|---|---|
| Mn(1)–O(1) | 2.271(4) | Mn(1)–O(5) | 2.124(3) |
| Mn(1)–O(2) | 2.238(4) | Mn(1)–O(6) | 2.128(4) |
| Mn(1)–O(3) | 2.245(3) | Mn(1)–O(7) | 2.135(4) |
| O(1)–Mn(1)–O(2) | 87.1(2) | O(2)–Mn(1)–O(7) | 171.1(1) |
| O(1)–Mn(1)–O(3) | 89.4(2) | O(3)–Mn(1)–O(5) | 160.0(1) |
| O(1)–Mn(1)–O(5) | 90.5(2) | O(3)–Mn(1)–O(6) | 90.1(1) |
| O(1)–Mn(1)–O(6) | 179.1(1) | O(3)–Mn(1)–O(7) | 100.7(1) |
| O(1)–Mn(1)–O(7) | 86.4(2) | O(5)–Mn(1)–O(6) | 90.2(1) |
| O(2)–Mn(1)–O(3) | 73.2(1) | O(5)–Mn(1)–O(7) | 99.2(1) |
| O(2)–Mn(1)–O(5) | 86.9(1) | O(6)–Mn(1)–O(7) | 92.9(1) |
| O(2)–Mn(1)–O(6) | 93.5(1) | | |

Hydrogen bonds

| A | H | B | A–H | H···B | A···B | A–H···B |
|---|---|---|---|---|---|---|
| O(1) | H(1) | N(2) | 0.97(8) | 2.76(8) | 2.98(1) | 94(5) |
| O(1) | H(2) | O(3) | 0.68(6) | 2.11(6) | 2.783(5) | 170(8) |
| N(1) | H(12) | O(7) | 0.95 | 2.27 | 3.16(1) | 156 |
| N(1) | H(13) | O(7) | 0.962 | 1.81 | 2.73(1) | 158 |
| N(2) | H(15) | O(7) | 0.92 | 2.54 | 2.87(1) | 102 |
| N(2) | H(16) | O(5) | 0.973 | 1.95 | 2.84(1) | 152 |

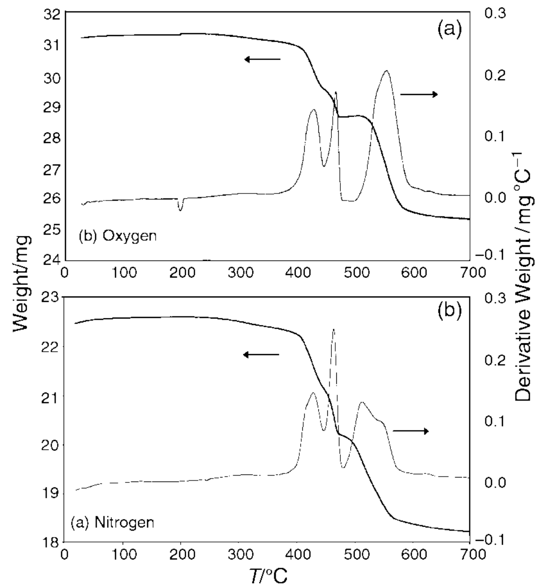


**Fig. 7** TGA plots of compound **1** under nitrogen (a) and oxygen (b) from room temperature to 700 °C at 10 °C min$^{-1}$.

the extra $O_2$ forms $Mn_2O_3$, however it was not possible to identify this from the powder pattern, and the mechanism of the decomposition is not clear.

### Magnetic measurements

The results of the magnetisation measurements on $[Mn_4(PO_4)_2(C_2O_4)(H_2O)_2]$ are shown in Fig. 8. At temperatures above approximately 40 K the susceptibility is characterised by simple Curie–Weiss behaviour with a paramagnetic Neél temperature, $\theta$, of −38.7 K and an effective moment per Mn ion $\mu_{eff}$ of 5.86 $\mu_B$, close to the expected free spin only $Mn^{2+}$ moment of 5.92 $\mu_B$. It is particularly interesting that although the Curie–Weiss behaviour found at high temperatures provides a clear indication of predominantly antiferromagnetic interactions, only a rounded maximum in the susceptibility is observed close to 15 K. The form of this broad maximum is typical of low dimensional antiferromagnetism as observed, for example, in the 2-D antiferromagnetic layered transition metal phosphonates, $[M^{II}(C_6H_5PO_3)(H_2O)]$.[26] The exciting possibility that the current compounds may represent a new family of low dimensional $S = 5/2$ antiferromagnets, in which there is weak magnetic coupling between the manganese tetramers *via* the phosphate or oxalate units, is currently being investigated.

### Relation to known structures

Other phosphate oxalate structures have recently been reported in tin,[27,28] aluminium,[20] gallium[21] and indium[22] systems. Of the transition metals, iron has been utilised in a number of structures[16–19] and vanadium in one,[29] however no manganese phosphate oxalates have previously been reported. Two of the iron frameworks have the same stoichiometry as that of **1**; the first of these was reported by us[16] and the second by Rao and co-workers,[17] is isostructural with **1**. TGA in air of this iron material showed a loss of water and oxalate, which resulted in a poorly crystalline material.

The two manganese materials reported here show structural features common to several other phosphate oxalates. Both **1** and **2** can be described as metal phosphate layers pillared by oxalate anions. Several other 3-D metal phosphate oxalates are described in the same way: $[C_4H_{12}N_2][In_2(HPO_4)_3(C_2O_4)]\cdot H_2O$,[22] $[Fe_4(PO_4)_2(C_2O_4)(H_2O)]$,[16] $[N_2C_4H_{12}]_{0.5}[Fe_2(HPO_4)(C_2O_4)_{1.5}]$, $[Fe_2(PO_4)(C_2O_4)_{0.5}(H_2O)]$,[17] $[NH_3(CH_2)_2NH_3]_{1.5}$-

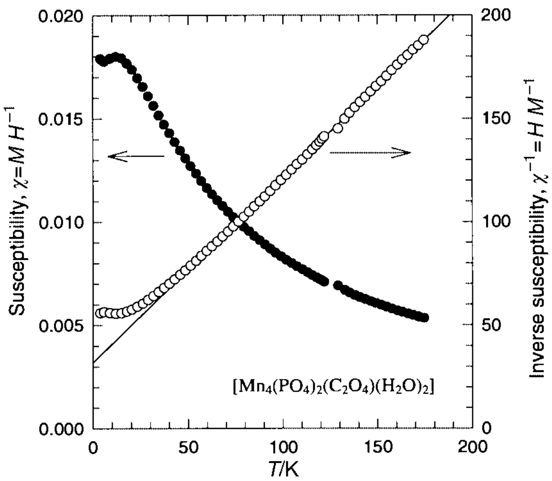


**Fig. 8** The susceptibility (closed circles) and inverse susceptibility (open circles) of $[Mn_4(PO_4)_2(C_2O_4)(H_2O)_2]$ measured in a magnetic field of 4 T (where $M$ = magnetisation, $H$ = applied field). Every tenth experimental point is plotted. The solid line represents the fit to the high temperature susceptibility of the Curie–Weiss form $C/(T - \theta)$ with $C = 1.1505$ K and $\theta = -38.7$ K.

$[Fe_3PO_4(HPO_4)_3(C_2O_4)_{1.5}]\cdot xH_2O$[18] and $[C_5H_{14}N_2][Fe_2(HPO_4)_3(C_2O_4)]$.[19] In contrast, $[Ga_5(OH)_2(C_{10}H_9N_2)(PO_4)_4(C_2O_4)]\cdot 2H_2O$[21] is constructed from $GaO_4$, $GaO_6$, $PO_4$ and oxalate sheets, with $GaO_4N$ polyhedra connecting the layers. Three different types of oxalate co-ordination are observed in the structures reported; monobidentate, bisbidentate, and bismono- and bis-bidentate. The monobidentate co-ordination is less common, seen in the one dimensional $[NH_3(CH_2)_2NH_3]_{2.5}[Al_4H(HPO_4)_4(H_2PO_4)_2(C_2O_4)_4]$[20] and $[C_4H_{12}N_2][VO(HPO_4)(C_2O_4)]$[29] where the anion caps the metal centre and allows hydrogen bonding between chains. It is the bisbidentate co-ordination of the oxalate anion bridging two metal centres, seen in other structures, which makes it an attractive candidate for use in open framework materials. Bismono- and bisbi-dentate co-ordination by the same oxalate anion results in three-co-ordinate oxygens, as observed in $[Fe_2(PO_4)(C_2O_4)_{0.5}(H_2O)]$[17] and **1**, leading to a continuous M–O–M linkage throughout the metal phosphate layers. Compound **1** has both bismono- and bisbi-dentate co-ordination, whereas **2** has only bisbi-dentate.

Two other phosphate oxalate materials show antiferromagnetic transitions: $[NH_3(CH_2)_2NH_3]_{1.5}[Fe_3(PO_4)(HPO_4)_3(C_2O_4)_{1.5}]\cdot xH_2O$[18] has $T_N = 31$ K, $\theta = -60$ K and $\mu_{eff} = 5.9\ \mu_B$, indicating high spin $Fe^{3+}$. The vanadium containing structure $[C_4H_{12}N_2][VO(HPO_4)(C_2O_4)]$[29] has a lower Neél temperature of 6 K. The compound $[N_2C_4H_{12}]_{0.5}[Fe_2(HPO_4)(C_2O_4)_{1.5}]$[17] shows a change in magnetic moment with temperature; the higher value (above 150 K) suggests $Fe^{2+}$ of intermediate spin ($t_g^5e_g^1$). The compound $[Fe_2(PO_4)(C_2O_4)_{0.5}(H_2O)]$, which is isostructural with **1**, shows Curie–Weiss behaviour ($\theta = -35.4$ K, $\mu = 5.15\ \mu_B$) but no $\chi$ maximum was observed.[17] Attempts have been made to synthesize a pure sample of **2**. The compounds $MnC_2O_4\cdot 2H_2O$, $H_3PO_4$ (aq), 1,3-diaminopropane and water in an approximate ratio 1 : 1 : 1 : 400 were heated at 120 °C for 48 hours, resulting in a pink product, which was predominantly **2** but also contained a small amount of $MnC_2O_4\cdot 2H_2O$ (JCPDS 25-544). Further attempts are ongoing.

## Conclusions

Two new three dimensional manganese phosphate oxalate frameworks, $[Mn_4(PO_4)_2(C_2O_4)(H_2O)_2]$ **1** and $[H_3N(CH_2)_3NH_3][Mn_2(HPO_4)_2(C_2O_4)(H_2O)_2]$ **2**, have been synthesized and their structures solved by single crystal X-ray diffraction. Thermogravimetric analysis of **1** indicates that the structure remains stable until around 240 °C, when water loss leads to structural collapse. The material shows predominantly antiferromagnetic interactions; a broad susceptibility maximum around 15 K may be evidence of low dimensional antiferromagnetism. Both structures are constructed from manganese phosphate layers bridged by oxalate groups, however **2** has a greater channel volume than **1** due to the presence of space filling 1,3-diaminopropane cations. It has not been possible to synthesize a pure sample of **2**; further work in this direction is in progress. We aim to develop this area of work by the use of different template species and alternative organic ligands, *e.g.* malonic acid.

## Acknowledgements

We thank the E.P.S.R.C. for a QUOTA studentship (Z. A. D. L.) and the University of St Andrews for support.

## References

1 M. E. Davis and R. F. Lobo, *Chem. Mater.*, 1992, **4**, 756.
2 S. L. Suib, *Chem. Rev.*, 1993, **93**, 803.
3 R. Szostak, *Molecular Sieves: Principles of Synthesis and Identification*, Van Nostrand Reinhold, New York, 1989.
4 T. Chirayil, P. Y. Zavalij and M. S. Whittingham, *Chem. Mater.*, 1998, **10**, 2629.
5 R. C. Haushalter and L. A. Mundi, *Chem. Mater.*, 1992, **4**, 31.
6 K.-H. Lii, Y.-F. Huang, V. Zima, C.-Y. Huang, H.-M. Lin, Y.-C. Jiang, F.-L. Liao and S.-L. Wang, *Chem. Mater.*, 1998, **10**, 2599.
7 M. Riou-Cavellec, D. Riou and G. Férey, *Inorg. Chim. Acta*, 1999, **291**, 317.
8 C. Janiak, *Angew. Chem., Int. Ed. Engl.*, 1997, **36**, 1431.
9 S. Kitagawa and M. Kondo, *Bull. Chem. Soc. Jpn.*, 1998, **71**, 1739.
10 P. Lightfoot and A. Snedden, *J. Chem. Soc., Dalton Trans.*, 1999, 3549.
11 S. S.-Y. Chui, S. M.-F. Lo, J. P. H. Charmant, A. G. Orpen and I. D. Williams, *Science*, 1999, **283**, 1148.
12 F. Serpaggi and G. Férey, *J. Mater. Chem.*, 1998, **8**, 2737.
13 O. M. Yaghi, G. M. Li and H. L. Li, *Nature* (*London*), 1995, **378**, 703.
14 M. A. Camblor, L. A. Villaescusa and M. J. Diaz-Cabañas, *Top. Catal.*, 1999, **9**, 59.
15 V. Patinec, P. A. Wright, P. Lightfoot, R. A. Aitken and P. A. Cox, *J. Chem. Soc., Dalton Trans.*, 1999, 3909.
16 Z. A. D. Lethbridge and P. Lightfoot, *J. Solid State Chem.*, 1999, **143**, 58.
17 A. Choudhury, S. Natarajan and C. N. R. Rao, *J. Solid State Chem.*, 1999, **146**, 538.
18 A. Choudhury, S. Natarajan and C. N. R. Rao, *Chem. Mater.*, 1999, **11**, 2316.
19 H.-M. Lin, K.-H. Lii, Y.-C. Jiang and S.-L. Wang, *Chem. Mater.*, 1999, **11**, 519.
20 P. Lightfoot, Z. A. D. Lethbridge, R. E. Morris, D. S. Wragg, P. A. Wright, Å. Kvick and G. B. M. Vaughan, *J. Solid State Chem.*, 1999, **143**, 74.
21 C.-Y. Chen, P. P. Chu and K.-H. Lii, *Chem. Commun.*, 1999, 1473.
22 Y.-F. Huang and K.-H. Lii, *J. Chem. Soc., Dalton Trans.*, 1998, 4085.
23 A. Altomare, M. C. Burla, M. Camalli, M. Cascarano, C. Giacovazzo, A. Gugliardi and G. Polidori, *J. Appl. Crystallogr.*, 1993, **26**, 343.
24 TEXSAN, Crystal Structure Analysis Package, Molecular Structure Corporation, Houston, TX, 1992.
25 I. D. Brown and D. Altermatt, *Acta Crystallogr., Sect. B: Struct. Sci.*, 1985, **41**, 244; A. S. Wills and I. D. Brown, VaList, Commissariat a l'Energie Atomique, France, 1999. Program available for the author at willsas@netscape.net.
26 J. Le Bideau, C. Payen, B. Bujoli, P. Palvadeau and J. Rouxel, *J. Magn. Magn. Mater.*, 1995, **140–144**, 1719.
27 S. Natarajan, *J. Solid State Chem.*, 1998, **139**, 200.
28 B. Adair, S. Natarajan and A. K. Cheetham, *J. Mater. Chem.*, 1998, **8**, 1477.
29 Y.-M. Tsai, S.-L. Wang, C.-H. Huang and K.-H. Lii, *Inorg. Chem.*, 1999, **38**, 4183.